Radiology technologies | Технологии лучевой диагностики

ISSN 1607-0763 (Print); ISSN 2408-9516 (Online)
https://doi.org/10.24835/1607-0763-1160

Accuracy of fat fraction estimation using Dixon: experimental phantom study

© **Olga Yu. Panina[1, 2, 4*], Alexander I. Gromov[2], Ekaterina S. Akhmad[1], Alexey V. Petraikin[1], Dmitry A. Bogachev[3], Dmitry S. Semenov[1], Anton V. Vladzymyrskyy[1], Yury A. Vasilev[1]**

[1] Research and Practical Clinical Center for Diagnostics and Telemedicine Technologies of Moscow Health Care Department; 24, Petrovka str., Moscow 127051, Russian Federation

[2] A.I. Evdokimov Moscow State University of Medicine and Dentistry of the Ministry of Healthcare of the Russian Federation; 20/1, Delegatskaya str., Moscow, 127473, Russian Federation

[3] Company with limited liability "EmulCom" , Russian Federation

[4] City Clinical Oncology Hospital No. 1; 17/1, Baumanskaya str., Moscow 105005, Russian Federation

Objective. Quantitative assessment of Dixon two-point and three-point technologies operation using phantom modeling in the range from 0 to 70%.

Materials and methods. To simulate substances with different concentrations of the fat phase we chose direct oil-in-water emulsions. Tubes with ready-made emulsions were placed in a phantom. Emulsions based on vegetable oils were presented in the range from 0–70%. The phantom was scanned on an Optima MR450w MRI tomograph (GE, USA) in two Dixon modes: the accelerated two-point method "Lava-Flex" and the three-point method "IDEAL IQ". A scan was performed on a GEM Flex LG Full RF coil. We calculated fat fraction (FF) using two formulas.

Results. There is a linear relationship of the determined values when calculating the fat concentration in "IDEAL IQ" mode and using the formula based on Water and Fat. The accuracy of body fat percentage measurement in "IDEAL IQ" mode is higher than in "Lava-Flex" mode. According to the MR-sequence "Lava-Flex" draws attention to the overestimation of the measured values of the concentration of fat in relation to the specified values by an average of 57.6% over the entire range, with an average absolute difference of 17.2%.

Conclusion. Using the "IDEAL IQ" sequence, the results of the quantitative determination of fractions by formulas were demonstrated, which are more consistent with the specified values in the phantom. In order to correctly quantify the fat fraction, it is preferable to calculate from the Water and Fat images using Equation 2. Calculations from the In-phase and Out-phase images provide ambiguous results. Phantom modeling with direct emulsions allowed us to detect the shift of the measured fat fraction.

Keywords: Fat quantification, phantom study, quality control, Dixon, magnetic resonance imaging

Conflict of interest. This study was prepared by research (No. in the EGISU: AAAA-A21-121012290079-2) under the Program of the Moscow Healthcare Department "Scientific Support of the Capital's Healthcare" for 2020–2022.

For citation: Panina O.Yu., Gromov A.I., Akhmad E.S., Petraikin A.V., Bogachev D.A., Semenov D.S., Vladzymyrskyy A.V., Vasilev Yu. A. Accuracy of fat fraction estimation using Dixon: experimental phantom study. *Medical Visualization.* 2022; 26 (4): 147–158. https://doi.org/10.24835/1607-0763-1160

Received: 22.03.2022. **Accepted for publication:** 01.07.2022. **Published online:** 20.10.2022.

Определение точности оценки фракции жира с использованием Dixon: экспериментальное фантомное исследование

© **Панина О.Ю.[1, 2, 4*], Громов А.И.[2], Ахмад Е.С.[1], Петряйкин А.В.[1], Богачев Д.А.[3], Семенов Д.С.[1], Владзимирский А.В.[1], Васильев Ю.А.[1]**

[1] ГБУЗ "Научно-практический клинический центр диагностики и телемедицинских технологий ДЗ города Москвы"; 127051 Москва, ул. Петровка, д. 24, стр. 1, Российская Федерация

[2] ФГБОУ ВО "Московский государственный медико-стоматологический университет им. А.И. Евдокимова" Минздрава России; 127473 Москва, ул. Делегатская, д. 20, стр.1, Российская Федерация

[3] ООО "ЭмульКом"; 124489 Московская обл., Елино, ул. Летняя, 1, Российская Федерация

[4] ГБУЗ города Москвы "Городская клиническая онкологическая больница №1 ДЗ города Москвы"; 105005 Москва, ул. Бауманская, д. 17/1, Российская Федерация

Цель исследования: оценка эффективности работы двухточечной и трехточечной МРТ-последовательностей Dixon при фантомном моделировании для определения жировой фракции в диапазоне от 0 до 70%.

Материал и методы. Для моделирования веществ с разной концентрацией жировой фазы были выбраны прямые эмульсии типа "масло в воде". Пробирки с эмульсиями помещались в цилиндрический фантом. Эмульсии на основе растительных масел были представлены в диапазоне от 0 до 70%. Сканирование выполнялось на МР-томографе 1,5 Тл Optima MR450w (GE, США). Было проведено сканирование в двух режимах Dixon: двухточечный метод "Lava-Flex" и трехточечный метод "IDEAL IQ". Было выполнено сканирование на РЧ-катушке GEM Flex LG Full. Фракция жира определялась расчетным методом.

Результаты. При расчете концентрации жира по данным последовательности "IDEAL IQ" по формуле, использующей данные изображений Water и Fat, определена линейная зависимость измеренных значений от заданных. Точность измерения процентного содержания жира в режиме "IDEAL IQ" выше, чем в режиме "Lava-Flex". По данным МР-последовательности "Lava-Flex" обращает на себя внимание завышение измеряемых значений концентрации жира по отношению к заданным в среднем на 57,6% на всем диапазоне при средней абсолютной разнице 17,2%.

Заключение. С помощью последовательности "IDEAL IQ" были продемонстрированы результаты количественного определения фракций по формулам, в большей степени соответствующие заданным величинам в фантоме. Для корректного количественного определения фракции жира предпочтительнее проводить расчеты по данным изображениям Water и Fat с использованием формулы (2). Расчеты по изображениям In-phase и Out-phase предоставляют неоднозначные результаты. Фантомное моделирование с использованием прямых эмульсий позволило определить смещение в значениях измеряемой фракции жира.

Ключевые слова: количественная оценка жировой ткани, фантомное исследование, контроль качества, Dixon, магнитно-резонансная томография

Конфликты интересов: статья подготовлена авторским коллективом в рамках научно-исследовательской работы (№ ЕГИСУ: АААА-А21-121012290079-2) в соответствии с Программой Департамента здравоохранения города Москвы "Научное обеспечение столичного здравоохранения" на 2020–2022 гг.

Для цитирования: Панина О.Ю., Громов А.И., Ахмад Е.С., Петряйкин А.В., Богачев Д.А., Семенов Д.С., Владзимирский А.В., Васильев Ю.А. Определение точности оценки фракции жира с использованием Dixon: экспериментальное фантомное исследование. *Медицинская визуализация.* 2022; 26 (4): 147–158. https://doi.org/10.24835/1607-0763-1160

Поступила в редакцию: 22.03.2022. **Принята к печати:** 01.07.2022. **Опубликована online:** 20.10.2022.

Introduction

Estimating the percentage of fat in tissues and organs on MRI images allows in some cases to shed light on the nature of the observed changes. This is made possible by the Dixon-type pulse sequence, widely available on the scanners from different manufacturers. The method relies on four sequences (water, fat, in-phase, out-phase) acquired in one scan. [1] In routine practice, the goal of using the Dixon out-phase sequences to assess the fat content is to confirm hepatic steatosis, to measure its degree, to enable diagnosis and differential diagnosis of adrenal lesions, to determine chylous tumours in the abdominal cavity, etc. [2]. Such capabilities are made possible by the special features of this technology, that allow to evaluate the fat amount inside the parenchymal organs or pathological formations.

The MR fat suppression technology in question is based on the works of Thomas Dixon and was named "Dixon" after the scientist [3]. A paper on the clinical application of this technique came out somewhat later [4]. The technology utilizes the fact that water and fat molecules precess at different rates (i.e. higher precess rate for water and lower for fat). This small gap is due to a difference in local magnetic fields – for water protons it is 220 Hz higher, while the field induction is 1.5T.

Figure 1 shows the principle behind the operation of this technique. Immediately after applying the initial excitation pulse α°, the water (blue arrow) and fat (yellow arrow) protons begin in-phase. Once a signal is registered after TE = 2.2 ms, the fat protons "move away" from the water protons and a signal becomes out-phase. Next, after 2TE, the motion of the fat protons triggers a second phasing of the spin system, and the protons of fat and water will again be in phase.

Over the past two decades, the academic interest in MRI fat quantification has grown substantially [5–7]. This can be explained by the fact, that at the moment scholars are searching for quantitative parameters that do not depend on data collection, platforms, scanner manufacturers, magnetic field induction, etc. Taken together, this may contribute to standardization and wide clinical application of the method in question [8]. In addition to routine practice, the fat quantification can be helpful in clinical trials during drug development [9,10]. However, a sufficient level of accuracy (low bias) and intermediate precision (low variability under different experimental conditions) of the quantitative metrics must be demonstrated [11].

In everyday practice, radiologists often lack confidence in determining the exact fat fraction percentage with certain tomography scanners, so the DIXON sequence is not always included in the scan protocols. Thus, the phantom modelling is there to help determining the accuracy of the quantitative data acquired using tomography scanners from various manufacturers.

Goal

Quantitative assessment of Dixon two-point and three-point methods using phantom modelling to assessing fat fractions in the range from 0 to 70%.

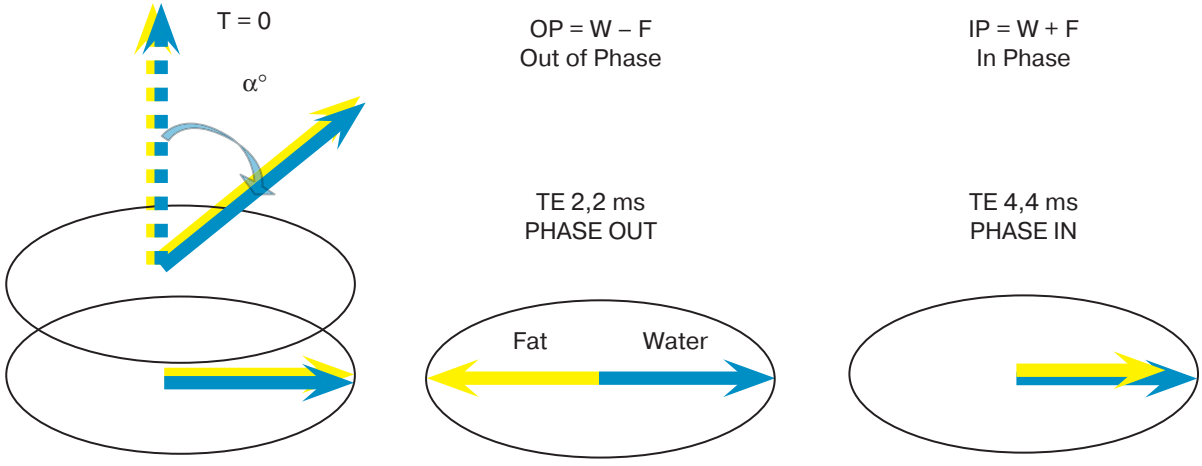

Fig. 1. Diagram of Dixon technology.

Materials and methods

Development of a physical model

The experiment utilized a phantom developed by the Center for Diagnostics and Telemedicine of the Moscow Healthcare Department (Fig. 2a). The phantom is a sealed acrylic cylinder with test tubes inside containing emulsions with the following fat phase concentrations: 0, 10%, 20%, 30%, 40%, 50%, 60%, 70% (Fig. 2a).

To simulate substances with various concentrations of the fat phase we chose direct oil-in-water emulsions. This model allows to combine two phases (water and fat) and evenly distribute one into the other [12].

The solutions were based on vegetable oils (sunflower and soybean) [13]. The BTMS (Behentrimonium Methosulfate) emulsifier was used to make a stable emulsion. To obtain a homogeneous and physically stable emulsion, we performed emulsification by heating the emulsifier, mixing it with vegetable oil and emulsifying it using an IKA Ultra Turrax T 25 Digital Homogenizer.

MR imaging protocol (phantom)

The phantom was scanned using a 1.5 T Optima MR450w MRI scanner (GE, the USA) with two Dixon modes: the accelerated two-point Lava Flex method and the three-point IDEAL IQ method (Iterative Decomposition of water and fat with Echo Asymmetry and Least-squares estimation). A scan was performed using a GEM Flex LG Full RF coil (Fig. 2b).

Lava-FLEX imaging parameters: TR – 7.58 s; TE (OUT/IN) – 2.084 s / 4.436 s; slice thickness – 5 mm; distance between slices – 5 mm; matrix – 256 × 256; the angle of inclination of the magnetization vector – 12°.

IDEAL IQ imaging parameters: TR – 13.507s; TE – 6.5 s; slice thickness – 5mm; slice increment – 2.5 mm; matrix – 160 × 160; inclination angle of magnetic field vector – 7°.

We measured the signal intensity on the In and Out images by establishing the region of interest (ROI) on the cross sections inside the tubes with different fat fraction values and preventing air from entering the region of interest.

Two well-known approaches were used to calculate the percentage of fat fractions (FF) [14]:
1 – a standard formula to mathematically combine the In and Out images:

$$FF1 = \frac{In - Out}{2In} \cdot 100\%, \quad (1)$$

2 – a formula that uses data from the Water and Fat images

$$FF2 = \frac{Fat}{Fat + water} \cdot 100\%, \quad (2)$$

Figure 3 shows MR images of the phantom in different phases: In-phase (In), Out-phase (Out) sequences, water-weighted (Water) and fat-weighted (Fat) sequences acquired using the Lava-Flex mode on a GEM Flex Coil. The first series shows the ROI order placed at the same level for all tubes and slices. Next, we compared the data calculated (measured) using both formulas with the default values of the fat concentration in the phantom. The obtained data are represented on diagrams (Fig. 4, 5).

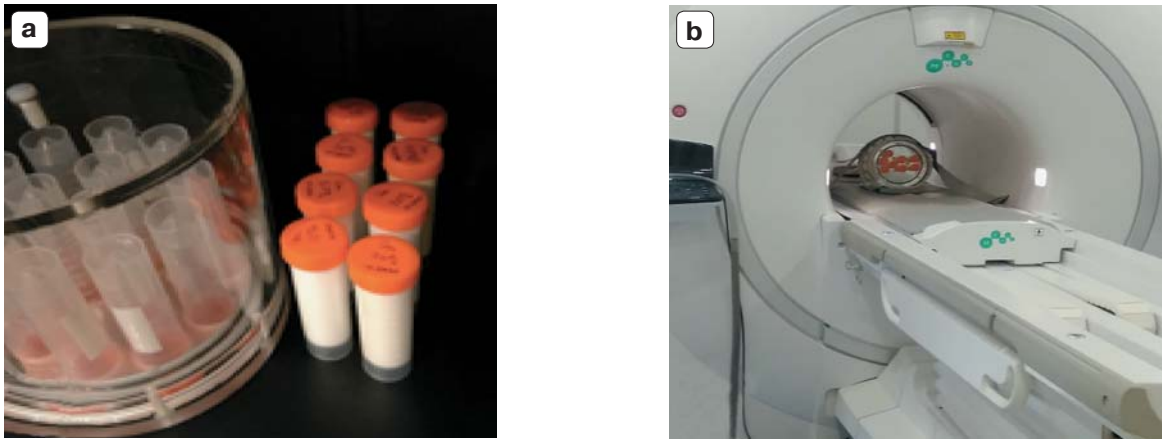

Fig. 2. Scheme of the experiment: **a** – installation of ready-made test tubes in a phantom; **b** – MRI examination of a phantom with a GEM Flex Body radiofrequency coil.

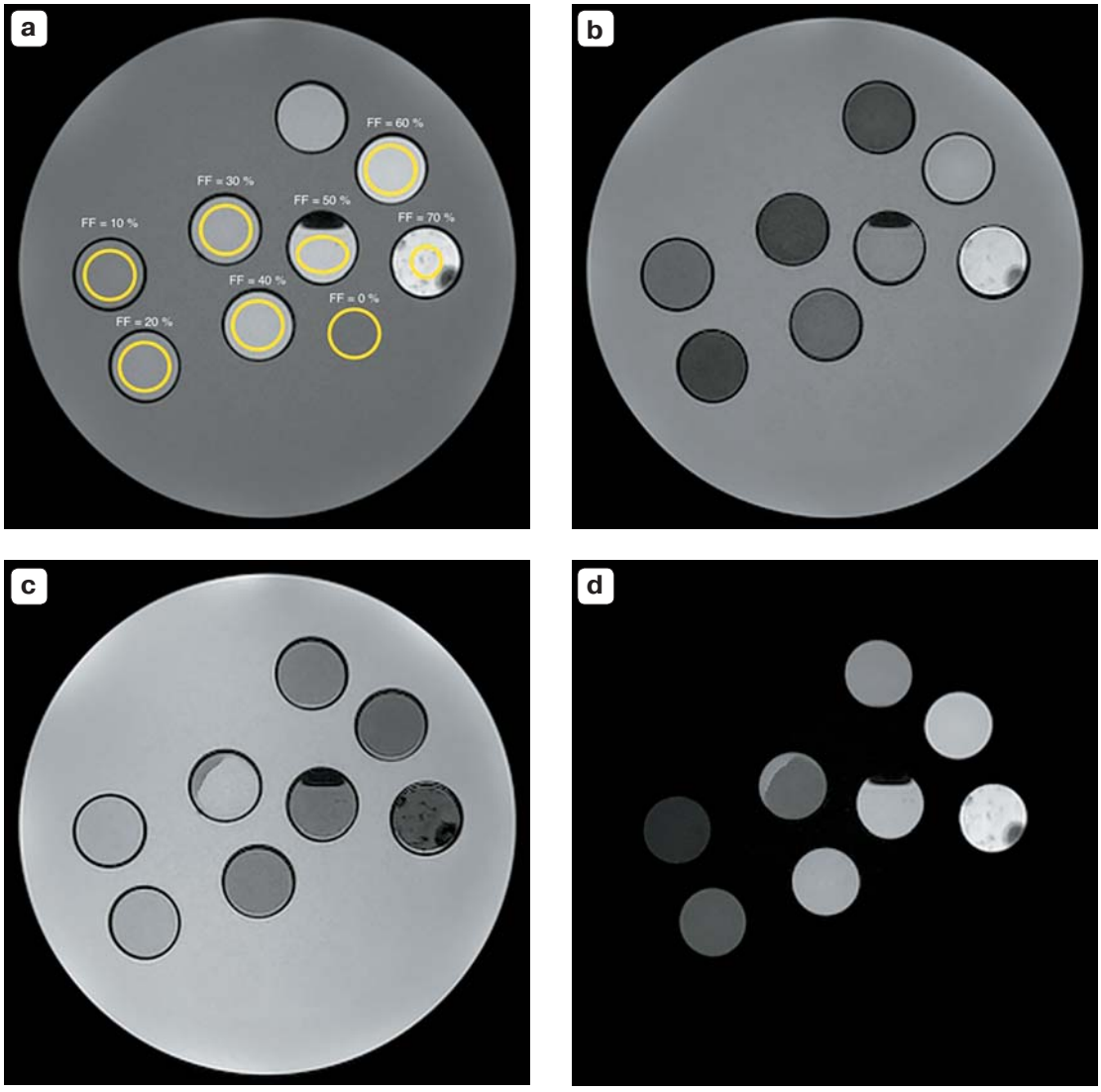

Fig. 3. MR images of the phantom in the "Lava-Flex" mode on the GEM Flex RF coil, abdominal. **a** – In-phase series with the designation ROI for data collection; **b** – Out-phase series; **c** – a series with signal intensity from Water; **d** – a series with signal intensity from Fat.

Results

Figures 4 and 5 show the results of the phantom scan in the Lava-Flex and IDEAL IQ modes. They reflect the mean value on the In-phase and Out-phase images (Fig. 4a, 5a) and compares the calculated vs. default fat concentration according to formulas 1 and 2 (Fig. 4b, 5b).

Lava-Flex

Since the In-phase images are T1-weighted, there is a linear increase in signal as the fat concentration goes up. At the same time, on the Out-phase images, an increase in the fat concentration is accompanied by a decrease in signal intensity in the range from 0 to 30%, with FF exceeding 30%. This means that the nature of the dependence changes to the opposite as the signal intensity increases (Fig. 4a). In this case, is should be possible to determine this minimum value at 50% fat concentration in the emulsion.

Comparison of the calculated fat fraction values revealed the following relationship. Formula (1) shows a linear relationship between the calculated and default fat concentrations, with a slight nonlinearity for FF = 20–30%. Where FF exceeds 30%, a gradual decrease in the calculated values is observed instead of an expected increase, i.e., an there is inflection when the values are 20% less than expected (50%). When using Formula (2), the dependence between

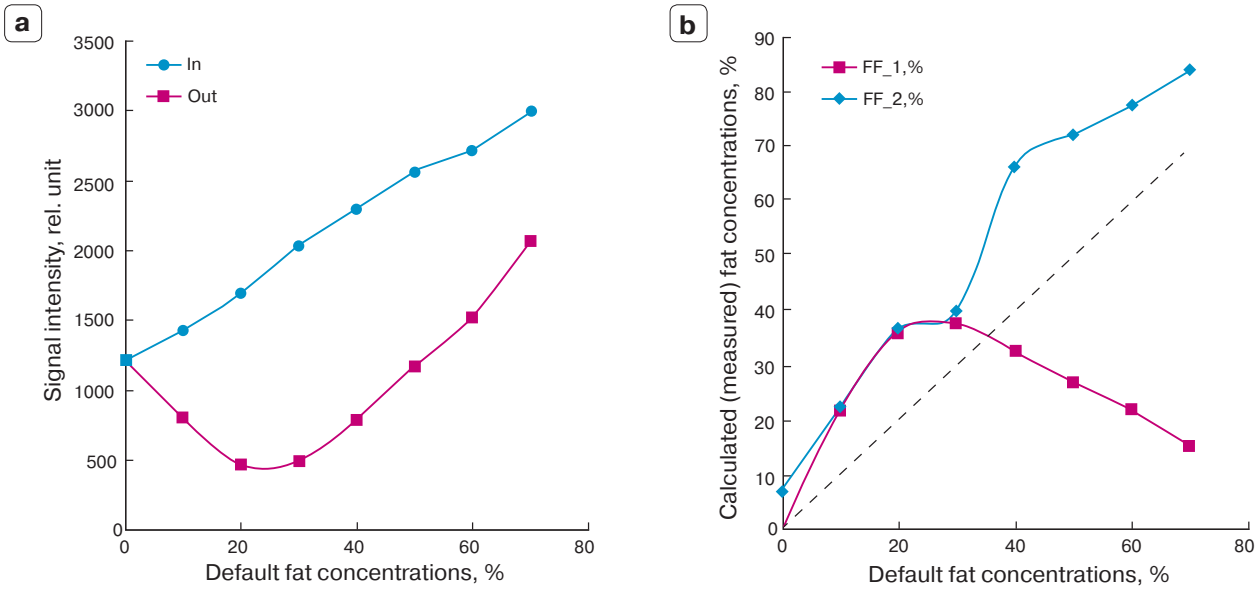

Fig. 4. The results of scanning the phantom in the "Lava-Flex" mode. **a** – the signal intensity on the images of the Out-phase and In-phase series at different values of fat concentration in the test tubes; **b** – comparison of the calculated (measured) and predetermined fat concentration according to formula (1) (FF_1) and (2) (FF_2). The horizontal line at approximately 22% demonstrates the possibility of relating two given fat concentrations to a given measured value.

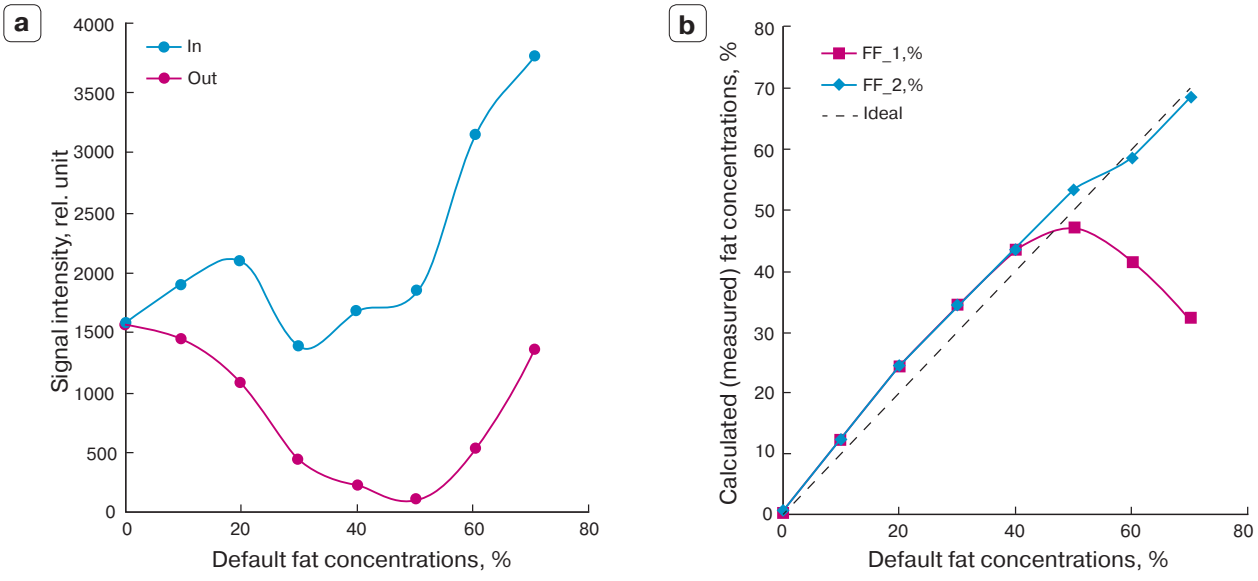

Fig. 5. The results of scanning the phantom in the "IDEAL" mode: **a** – signal intensity on the images of the Out-phase and In-phase series at different values of fat concentration in the test tubes; **b** – comparison of the calculated (measured) and predetermined fat concentration according to formula (1) (FF_1) and (2) (FF_2).

the calculated and default fat concentrations is observed in the presence of a pronounced nonlinearity in the range FF = 20–40%. There is an upward bias of the fat concentration values in relation to the default values by an average of 57.6% over the entire range, with an average absolute difference of 17.2% (Fig. 4b).

IDEAL IQ

This sequence also ensures T1-weighting and a non-linear dependence of the signal from the fat concentration on the In-phase images. A signal decrease is observed in the range FF = 30–50%. When scanning the phantom using the Out-phase mode, a dependence was noted corresponding to the expected behaviour of the signal. At FF = 50%, the signal hits its lowest point (Fig. 5a). This happens because the signals from water and fat cancel each other out on the Out-phase, provided the fat and water concentrations are the same. Although the dependence of the signal intensity on the In-phase is non-linear, the results of the quantitative measurement of the fractions using the formulas are more consistent with the default values, compared to Lava-Flex.

When using Formula (1), there is a strong linear dependence between the calculated and default values of the fat concentration in the range of FF 0-50%, followed by a gradual decrease in the calculated values away from the expected ones. When calculating according to Formula (2), there is an almost complete agreement between the calculated and true fat concentrations (the average relative error is 9.7%, and the absolute difference in fat concentration is 2.0%) within the entire FF range (Fig. 5b). Thus, both methods yield a good agreement between the calculated and default values.

The difference between the minimum value on the Out-phase diagram and the maximum value of the fat concentration calculated using the Formula (1) for Lava-flex is 6.0%. For IDEAL IQ, this difference is 1.0%.

A number of tomography scanners are capable of making images in In-phase and Out-phase modes only. For these data it is suggested to use Formula (1). At the same time, there is an uncertainty in the assessment of the fat fraction, since two fat/water ratios can be corresponding to the same calculated value (Fig. 4 b).

Clinical case study

A 53-year-old woman was admitted to Medsi Clinical Hospital 2 with a diagnosis of retroperitoneal neoplasm. Abdominal CT (Fig. 6) of the tail of the pancreas revealed a pathological mass of 5 × 4 × 4 cm in size with fat density –35 HU. Ultrasound and MRI scans also suggested a retroperitoneal lipoma.

The MRI imaging of the root of mesentery was performed to detect a pathological mass with thickened walls. Its content showed high signal intensity on T2-WI images, and a partial suppression of the signal on T2FS-WI (Fig. 7). The Lava-Flex mode (Dixon) showed a high signal intensity on Fat images, low on Water, a slightly lower intensity compared to the fat tissue on In-phase images, and a decrease in signal on Out-phase. The obtained signal characteristics indicate that the cyst consists of fatty emulsion.

A decrease in signal intensity was registered in the Out-phase images (e) compared to the In-phase images (c). Formula (2) that take into account the signal intensity for Fat and Water (798 and 237, respectively), detected a fat content of 77.1%. Calculation of the fat fraction using Formula (1) that takes into account the signal intensity for In-phase and Out-phase (1191 and 742, respectively), detected a fat content of 18.8%. According to the results obtained in phantom, the calculated value of 18.8% may correspond to the second value of the default fat fraction concentration with a higher fat content of 65%, which is much closer to the Formula (2) results (Fig. 4b). It has been suggested that this mass is a chylous cyst of the mesentery with a high fat fraction content.

Operative confirmation: a tumour 5 × 4 × 4 cm in size was detected in the root of the mesentery near the ligament of Treitz (Fig. 8a). The tumour was removed and the proximal

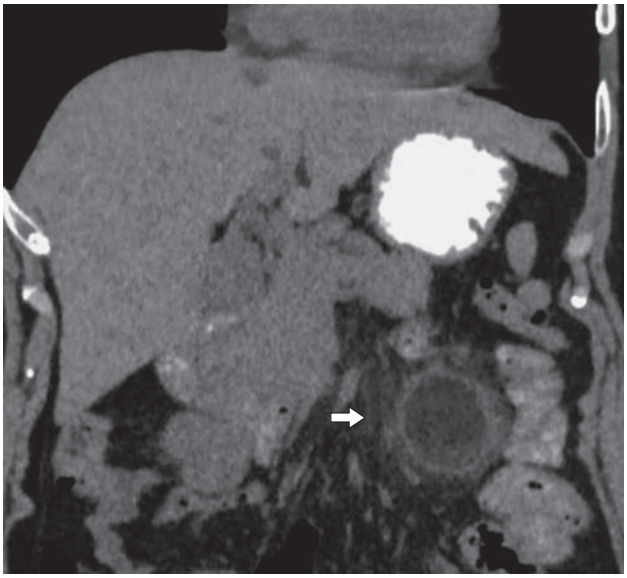

Fig. 6. CT scan of the abdomen, coronal section. Encapsulated formation of fat density in the region of the root of the mesentery of the small intestine (arrow).

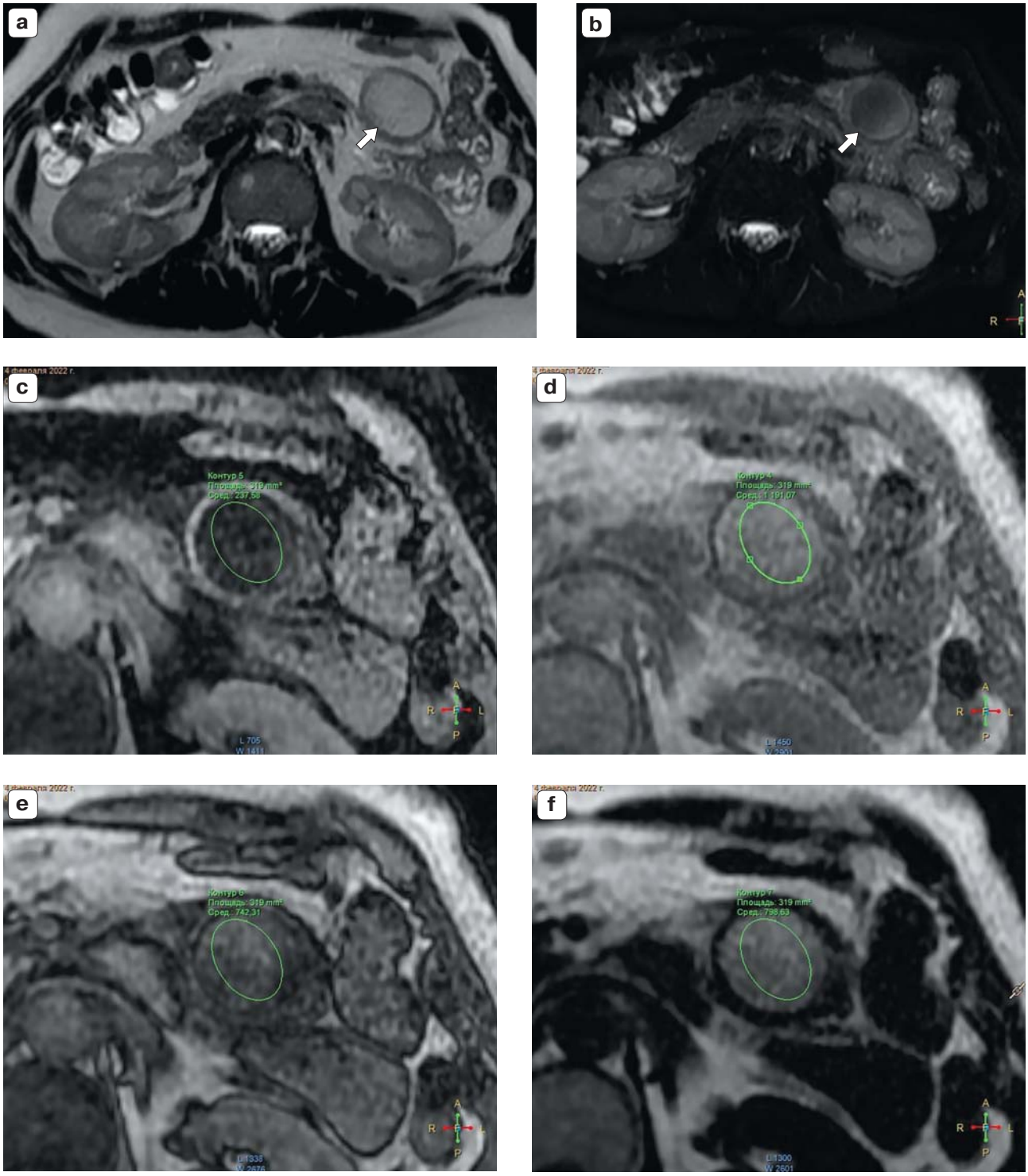

Fig. 7. Magnetic resonance imaging, axial section. **a** – T2-WI – thick-walled pathological formation in the root of the mesentery of the small intestine with a moderately high intensity of the MR signal (arrow). **b** – T2-WI FS shows suppression of the signal by part of the lesion (arrow); **c–f** – Lava-Flex mode: **c**– water; **d** – In-phase; **e** – Out-phase; **f** – Fat. Ellipse – ROI area of interest for determining signal intensity values.

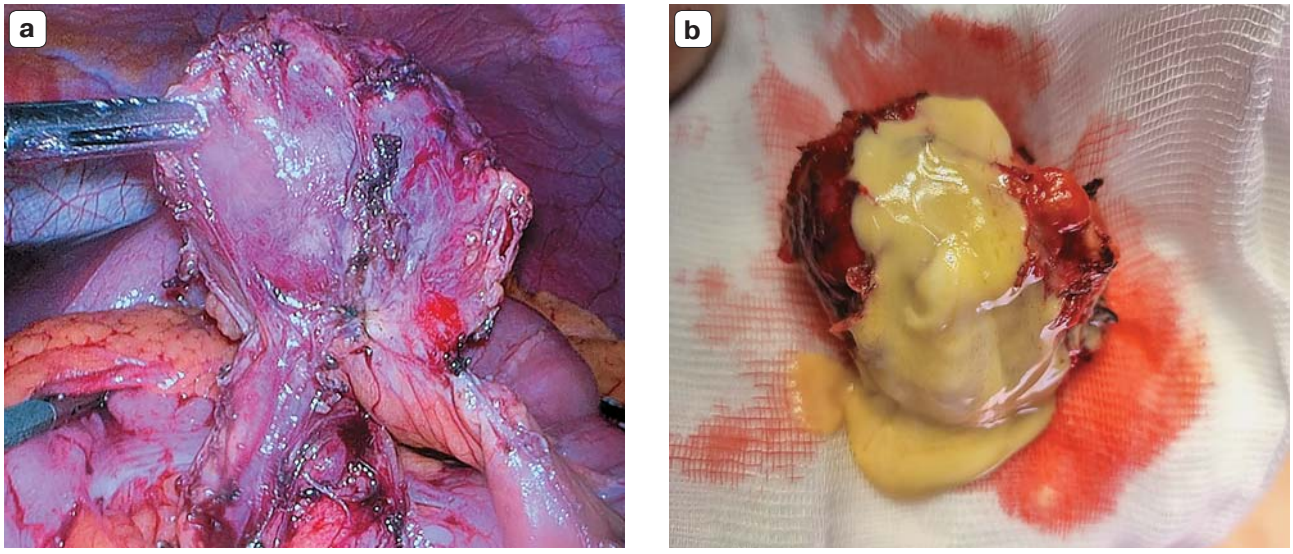

Fig. 8. Gross specimen of a distant lesion. **a** – pathological formation at laparoscopy; **b** – appearance of the preparation after removal of the walls.

mesenteric arteries were preserved. The surgical specimen contained a thick-walled cystic mass. When cut, the content was white and yellow, partly dense and casseous, partly – emulsion-like liquid (Fig. 8b). The liquid content was collected inside a container (Fig. 8c).

In addition, we analysed the liquid part of the cyst (presented as emulsion), with an MRI ex vivo scan in the Lava-Flex mode. A similar decrease in signal intensity was registered on the In-phase images compared to the Out-phase images (c). The following data on the fat fraction percentage were obtained using Formula (1): 31,8%. According to the rationale above, the calculated fat concentration could also be 45%, while Formula (2) suggests 64,3%.

This clinical observation demonstrates a type of a chylous cyst in the mesentery with a high fat content (over 50%). Using the formula to calculate the fat fraction that take into account the Fat and Water image data, turned out to be more consistent with the actual measurements. The use of a more common formula that takes into account the In / Out-phase image data yielded ambiguous values of the fat concentration. The phantom modelling helped to identify and partially correct the observed discrepancies.

Discussion

This paper assessed the linearity of the findings delivered by the two-point method Lava Flex and the three-point method IDEAL IQ with regard to the fat fraction concentration. Lava Flex is a two-point Dixon T1-weighted In phase and Out phase gradient echo sequences (GRE) that automatically create fat-only (FAT) and water-only (WATER) image sets, and is widely available on most MR scanners [15]. IDEAL IQ, being somewhat similar to the Lava Flex Dixon sequence, features echo asymmetry with an iterative least squares estimation algorithm that improves the signal-to-noise ratio [16].

The results provide evidence both for possible inconsistency of the declared imaging parameters and the need to control the quality of the MR pulse sequences. The observed changes highlighted an inconsistency between the Lava Flex and IDEAL IQ modes. Calculation of the fat concentration in IDEAL IQ mode using the formula that took data from the Water and Fat images (Formula (2)) revealed a linear relationship between the default and measured values. The formula that utilises the In-phase and Out-phase data (Formula (1)) can be used to calculate the fat concentration only in the range from 0 to 50%. Thus, if the fat concentration is greater than 50%, it is necessary to tailor the formula and introduce adjustment factors. However, to determine the cause of such changes and develop specific practical recommendations to fine tune the Dixon modes, it is necessary to continue the experimental part of this work, and to study the clinical application of the results above.

MRI is sensitive to a number of factors that can influence the assessment of fat tissue. These includes the difference in T1 relaxation time between fat and water, T2* shifts, phase errors, temperature effects, the presence of hemosiderin in tissues, etc. [11,17]. Non-linearity and deviation of values during the quality control and sequencing can be detected

using phantoms. Academic literature provides examples of using the phantom modelling for quality control of pulse sequences, particularly for the Dixon method [9,18].

In particular, Fischer et al. used a phantom with FF from 0-100% containing muscle and fat of animal origin, that demonstrated advantages of the two-point Dixon method vs. visual assessment of fat volume in calf muscles [9]. Another study used a 0–70% FF phantom with a mixture of peanut oil and hydroxyapatite to investigate the changes in fat and water concentrations in pathological conditions affecting the bone marrow, including spondylarthritis, osteomyelitis, tumours and fractures. The study demonstrated a linear relationship between the measured and true values with the measurement error below 10% [10]. To assess the accuracy and precision of FF measurements on several scanners with different magnetic field strengths, Hernando et al. used a fat-water phantom with FF concentrations ranging from 0-50% and 100% containing a mixture of peanut oil and agar. As a result, the study showed a linear dependence between the measured and the true values with a minimal measurement error [11]. A similar experiment was carried out using a phantom with FF from 0–50% and 100% [19]. Another study utilized a phantom with a FF concentrations of 0–50% containing a mixture of soybean and rapeseed oils [18]. However, the above-mentioned studies utilized FF concentrations below 50%. A distinctive feature of our phantom was the FF concentrations of 0–70% (including 50% and 60%) that were based on vegetable oils (i.e. sunflower and soybean).

A limitation in this paper was the lack of tubes with FF greater than 70%. This was due to the fact that when trying to use this method to prepare emulsions with over 70% fat fraction, the emulsion separated into fat and water, while the assessment of signal characteristics requires a homogeneous emulsion.

Thus, the phantom described in the paper, makes it possible to secure the intermediate precision of measurements across different tomography scanners, to validate the results and to ensure quality control regardless of the manufacturer and model.

Conclusions

Phantom modeling using the oil-in-water emulsions made it possible to evaluate the opportunities offered by quantitative measurement of the fat fraction using the Dixon sequences. The accuracy of the body fat percentage measurement in IDEAL IQ mode is higher compared to the Lava-Flex mode. Using the IDEAL IQ sequence, we demonstrated the results of the formula-based quantitative measurement of FF, which happened to be more consistent with the default values in the phantom. In order to accurately quantify the fat fraction, the calculations should be based on Formula (2) that takes data from Water and Fat images. Calculations from the In-phase and Out-phase images yield ambiguous results. Improving the phantom studies would allow to ensure proper quality control of MRI studies. In future, the precision factor would also help to develop the standards for the fat tissue assessment that could be used to establish accurate diagnosis and perform measurements.

Acknowledgements

The authors would like to thank to S.V. Shalimov (Gray Safe LLC, Moscow, Russia) and M.S. Aimanov (Gamma NPP, Almaty, Kazakhstan) for their assistance in the production of the phantom.

Funding

This study was prepared by research (No. in the EGISU: AAAA-A21-121012290079-2) under the Program of the Moscow Healthcare Department “Scientific Support of the Capital’s Healthcare” for 2020–2022.

Authors’ participation

Panina O.Y. – conducting research, collection and analysis of data, writing text, responsibility for the integrity of all parts of the article.

Gromov A.I. – concept and design of the study, analysis and interpretation of the obtained data, text preparation and editing.

Akhmad E.S. – conducting research, collection and analysis of data, writing text, statistical analysis.

Petraikin A.V. – analysis and interpretation of the obtained data, approval of the final version of the article.

Bogachev D. A. – preparation of the material part of the experiment.

Semenov D.S. – participation in scientific design , approval of the final version of the article.

Vladzymyrskyy A.V. – approval of the final version of the article.

Vasilev Yu.A. – approval of the final version of the article.

References

1. Van Vucht N., Santiago R., Lottmann B. et al. The Dixon technique for MRI of the bone marrow. *Skeletal Radiol*. 2019; 48 (12): 1861–1874. https://doi.org/10.1007/s00256-019-03271-4.
2. Gromov A.I., Gorinov A.V., Galljamov E.A. Mesenteric chillous lymphangioma. Visualization features on opposed-phase MR images. *Medical Visualization*. 2019; 23 (4): 86–92. https://doi.org/10.24835/1607-0763-2019-4-86-92 (In Russian)
3. Dixon W.T. Simple proton spectroscopic imaging. *Radiology*. 1984; 153. https://doi.org/10.1148/radiology.153.1.6089263

4. Outwater E.K., Blasbalg R., Siegelman E.S., Vala M. Detection of Lipid in Abdominal Tissues with Opposed-Phase Gradient-Echo Images at 1.5 T: Techniques and Diagnostic Importance. *Radiographics*. 1998; 18. https://doi.org/10.1148/radiographics.18.6.9821195
5. Serai S.D., Dillman J.R., Trout A.T. Proton density fat fraction measurements at 1.5- and 3-T hepatic MR imaging: Same-day agreement among readers and across two imager manufacturers. *Radiology*. 2017; 284. https://doi.org/10.1148/radiol.2017161786
6. Schmeel F.C., Vomweg T., Träber F. et al. Proton density fat fraction MRI of vertebral bone marrow: Accuracy, repeatability, and reproducibility among readers, field strengths, and imaging platforms. *J. Magn. Reson. Imaging*. 2019; 50. https://doi.org/10.1002/jmri.26748
7. Lohöfer F.K., Kaissis G.A., Müller-Leisse C. et al. Acceleration of chemical shift encoding-based water fat MRI for liver proton density fat fraction and T2 mapping using compressed sensing. *PLoS One*. 2019; 14. https://doi.org/10.1371/journal.pone.0224988
8. Reeder S.B., Hu H.H., Sirlin C.B. Proton density fat-fraction: A standardized mr-based biomarker of tissue fat concentration. *J. Magn. Reson. Imaging*. 2012; 36. https://doi.org/10.1002/jmri.23741
9. Fischer M.A., Pfirrmann C.W.A., Espinosa N. et al. Dixon-based MRI for assessment of muscle-fat content in phantoms, healthy volunteers and patients with achillodynia: Comparison to visual assessment of calf muscle quality. *Eur. Radiol.* 2014; 24: 1366–1375. https://doi.org/10.1007/s00330-014-3121-1
10. Bainbridge A., Bray T.J.P., Sengupta R., Hall-Craggs M.A. Practical Approaches to Bone Marrow Fat Fraction Quantification Across Magnetic Resonance Imaging Platforms. *J. Magn. Reson. Imaging*. 2020; 52: 298–306. https://doi.org/10.1002/jmri.27039
11. Hernando D., Sharma S.D., Aliyari Ghasabeh M. et al. Multisite, multivendor validation of the accuracy and reproducibility of proton-density fat-fraction quantification at 1.5T and 3T using a fat-water phantom. *Magn. Reson. Med*. 2017; 77: 1516–1524. https://doi.org/10.1002/mrm.26228
12. Sergunova K.A. The use of reverse emulsion based on siloxanes to control the measured diffusion coefficient in magnetic resonance imaging. *Biomedical Engineering*. 2019; 5: 22–25. (In Russian)
13. Morozov S., Sergunova K., Petraikin A. et al. Diffusion processes modeling in magnetic resonance imaging. *Insights Imaging*. 2020; 11. https://doi.org/10.1186/s13244-020-00863-w
14. Bhat V., Velandai S., Belliappa V. et al. Quantification of Liver Fat with mDIXON Magnetic Resonance Imaging, Comparison with the Computed Tomography and the Biopsy. *J. Clin. DIAGNOSTIC. Res*. 2017;11:TC06.
15. Samji K., Alrashed A., Shabana W.M. et al. Comparison of high-resolution T1W 3D GRE (LAVA) with 2-point Dixon fat/water separation (FLEX) to T1W fast spin echo (FSE) in prostate cancer (PCa). *Clin. Imaging*. 2016; 40. https://doi.org/10.1016/j.clinimag.2015.11.023
16. Reeder S.B., Pineda A.R., Wen Z. et al. Iterative decomposition of water and fat with echo asymmetry and least-squares estimation (IDEAL): Application with fast spin-echo imaging. *Magn. Reson. Med*. 2005; 54: 636–644. https://doi.org/10.1002/mrm.20624
17. Labranche R., Gilbert G., Cerny M. et al. Liver iron quantification with MR imaging: A primer for radiologists. *Radiographics*. 2018; 38. https://doi.org/10.1148/rg.2018170079
18. Hayashi T., Fukuzawa K., Yamazaki H. et al. Multicenter, multivendor phantom study to validate proton density fat fraction and T2* values calculated using vendor-provided 6-point DIXON methods. *Clin. Imaging*. 2018; 51: 38–42. https://doi.org/10.1016/j.clinimag.2018.01.011
19. Hutton C., Gyngell M.L., Milanesi M. et al. Validation of a standardized MRI method for liver fat and T2 quantification. *PLoS One*. 2018; 13. https://doi.org/10.1371/journal.pone.0204175

Contact*: Olga Yu. Panina – E-mail: olgayurpanina@gmail.com; o.panina@npcmr.ru

Olga Yu. Panina – Junior Scientist Researcher of Technical Monitoring and QA Development Department, Research and Practical Clinical Center for Diagnostics and Telemedicine Technologies of Moscow Health Care Department; MD, radiologist, City Clinical Oncological Hospital No. 1 of Moscow Health Care Department; senior laboratory assistant, Moscow State University of Medicine and Dentistry named after A.I. Evdokimov, Moscow. https://orcid.org/0000-0002-8684-775X;

Alexander I. Gromov – Doct. of Sci. (Med.), Associate Professor, A.I. Evdokimov Moscow State University of Medicine and Dentistry of the Ministry of Healthcare of the Russian Federation; head of the radiation diagnosis and treatment methods, Oncourology Department, Moscow. https://orcid.org/0000-0002-9014-9022

Ekaterina S. Akhmad – Scientist Researcher of Technical Monitoring and QA Development, Research and Practical Clinical Center for Diagnostics and Telemedicine Technologies of Moscow Health Care Department, Moscow. https://orcid.org/0000-0002-8235-9361

Alexey V. Petraikin – Cand. of Sci. (Med.), Associate Professor, Senior Researcher of Technical Monitoring and QA Development, Research and Practical Clinical Center for Diagnostics and Telemedicine Technologies of Moscow Health Care Department, Moscow. https://orcid.org/0000-0003-1694-4682

Dmitry A. Bogachev – Head of the laboratory "EmulCom" company, Moscow region.

Dmitry S. Semenov – Scientist Researcher of Technical Monitoring and QA Development, Research and Practical Clinical Center for Diagnostics and Telemedicine Technologies of Moscow Health Care Department, Moscow. https://orcid.org/0000-0002-4293-2514

Anton V. Vladzymyrskyy – Doct. of Sci. (Med.), Associate Professor, Deputy Director for Science, Research and Practical Clinical Center for Diagnostics and Telemedicine Technologies of Moscow Health Care Department, Moscow. https://orcid.org/0000-0002-2990-7736

Yury A. Vasilev – Cand. of Sci. (Med.), Director, Research and Practical Clinical Center for Diagnostics and Telemedicine Technologies of Moscow Health Care Department, Moscow. https://orcid.org/0000-0002-0208-5218

Для корреспонденции*: Панина Ольга Юрьевна – 127051 Москва, ул. Петровка, д. 24. Тел.: +7-926-621-01-79.
E-mail: olgayurpanina@gmail.com; o.panina@npcmr.ru

Панина Ольга Юрьевна – младший научный сотрудник отдела инновационных технологий ГБУЗ "Научно-практический клинический центр диагностики и телемедицинских технологий ДЗ города Москвы"; старший лаборант кафедры лучевой диагностики ФГБОУ ВО "Московский государственный медико-стоматологический университет им. А.И. Евдокимова" Минздрава России; врач-рентгенолог ГКОБ №1 ДЗ города Москвы, Москва. https://orcid.org/0000-0002-8684-775X

Громов Александр Игоревич – доктор мед. наук, профессор, профессор кафедры лучевой диагностики ФГБОУ ВО "Московский государственный медико-стоматологический университет им. А.И. Евдокимова" Минздрава России, Москва.
https://orcid.org/0000-0002-9014-9022

Ахмад Екатерина Сергеевна – младший научный сотрудник отдела инновационных технологий ГБУЗ "Научно-практический клинический центр диагностики и телемедицинских технологий ДЗ города Москвы", Москва. https://orcid.org/0000-0002-8235-9361

Петряйкин Алексей Владимирович – канд. мед. наук, ведущий научный сотрудник отдела инновационных технологий ГБУЗ "Научно-практический клинический центр диагностики и телемедицинских технологий ДЗ города Москвы", Москва.
https://orcid.org/0000-0003-1694-4682

Богачев Дмитрий Александрович – руководитель лаборатории ООО "ЭмульКом", Московская обл.

Семенов Дмитрий Сергеевич – научный сотрудник отдела инновационных технологий ГБУЗ "Научно-практический клинический центр диагностики и телемедицинских технологий ДЗ города Москвы", Москва. https://orcid.org/0000-0002-4293-2514

Владзимирский Антон Вячеславович – доктор мед. наук, профессор, заместитель директора по научной работе ГБУЗ "Научно-практический клинический центр диагностики и телемедицинских технологий ДЗ города Москвы", Москва. https://orcid.org/0000-0002-2990-7736

Васильев Юрий Александрович – канд. мед. наук, директор ГБУЗ "Научно-практический клинический центр диагностики и телемедицинских технологий ДЗ города Москвы", Москва. https://orcid.org/0000-0002-0208-5218